

# Regulatory Roles of Anoctamin-6 in Human Trabecular Meshwork Cells

Juni Banerjee,<sup>1</sup> Chi-Ting Leung,<sup>1</sup> Ang Li,<sup>1,2</sup> Kim Peterson-Yantorno,<sup>1</sup> Huan Ouyang,<sup>2</sup> W. Daniel Stamer,<sup>3</sup> and Mortimer M. Civan<sup>1,4</sup>

<sup>1</sup>Department of Physiology, University of Pennsylvania Perelman School of Medicine, Philadelphia, Pennsylvania, United States

<sup>2</sup>Guangdong-Hong Kong - Macau Institute of CNS Regeneration, Guangdong Key Laboratory of Brain Function and Diseases, Jinan University, Guangzhou, China

<sup>3</sup>Departments of Ophthalmology and Biomedical Engineering, Duke University, DUMC 3802, Durham, North Carolina, United States

<sup>4</sup>Department of Medicine, University of Pennsylvania Perelman School of Medicine, Philadelphia, Pennsylvania, United States

Correspondence: Mortimer M. Civan, Department of Physiology, University of Pennsylvania Perelman School of Medicine, 715A Clinical Research Building, 415 Curie Boulevard, Philadelphia, PA 19104-6085, USA; civan@mail.med.upenn.edu.

Submitted: June 23, 2016

Accepted: December 7, 2016

Citation: Banerjee J, Leung C-T, Li A, et al. Regulatory roles of anoctamin-6 in human trabecular meshwork cells. *Invest Ophthalmol Vis Sci*. 2017;58:492–501. DOI:10.1167/iov.16-20188

**PURPOSE.** Trabecular meshwork (TM) cell volume is a determinant of aqueous humor outflow resistance, and thereby IOP. Regulation of TM cell volume depends on chloride ion ( $\text{Cl}^-$ ) release through swelling-activated channels ( $I_{\text{Cl,Swell}}$ ), whose pore is formed by LRRC8 proteins. Chloride ion release through swelling-activated channels has been reported to be regulated by calcium-activated anoctamins, but this finding is controversial. Particularly uncertain has been the effect of anoctamin An6, reported as a  $\text{Ca}^{2+}$ -activated  $\text{Cl}^-$  (CaCC) or cation channel in other cells. The current study tested whether anoctamin activity modifies volume regulation of primary TM cell cultures and cell lines.

**METHODS.** Gene expression was studied with quantitative PCR, supplemented by reverse-transcriptase PCR and Western immunoblots. Currents were measured by ruptured whole-cell patch clamping and volume by electronic cell sizing.

**RESULTS.** Primary TM cell cultures and the TM5 and GTM3 cell lines expressed An6 3 to 4 orders of magnitude higher than the other anoctamin CaCCs (Ano1 and Ano2). Ionomycin increased cell  $\text{Ca}^{2+}$  and activated macroscopic currents conforming to CaCCs in other cells, but displayed significantly more positive mean reversal potentials (+5 to +12 mV) than those displayed by  $I_{\text{Cl,Swell}}$  (–14 to –21 mV) in the same cells. Nonselective CaCC inhibitors (tannic acid >  $\text{CaCC}_{\text{inh-A01}}$ ) and transient An6 knockdown strongly inhibited ionomycin-activated currents,  $I_{\text{Cl,Swell}}$  and the regulatory volume response to hyposmotic swelling.

**CONCLUSIONS.** Ionomycin activates CaCCs associated with net cation movement in TM cells. These currents,  $I_{\text{Cl,Swell}}$ , and cell volume are regulated by An6. The findings suggest a novel clinically-relevant approach for altering cell volume, and thereby outflow resistance, by targeting An6.

**Keywords:** TMEM16F,  $I_{\text{Cl,Swell}}$ , regulatory volume decrease, calcium-activated  $\text{Cl}^-$  current, intraocular pressure, outflow facility

**G**laucoma usually is associated with increased resistance (decreased outflow facility) of aqueous humor flow through the conventional trabecular outflow pathway.<sup>1,2</sup> For outflow to match inflow in glaucoma, IOP must rise to overcome the increased outflow resistance. The elevated IOP leads to death of retinal ganglion cells and optic atrophy. If optic atrophy is caused by elevated outflow resistance, the most direct intervention would be to lower trabecular outflow resistance.

Among other modulators of outflow,<sup>3,4</sup> cell volume within the trabecular meshwork (TM) pathway is linked to outflow resistance. Volume changes of TM, juxtacanalicular, and Schlemm canal cells produce transient changes in outflow resistance of human, nonhuman primate, and calf eyes.<sup>5–7</sup> These changes occur within approximately 15 minutes,<sup>5,7</sup> probably by distorting optimal fluid funneling in the juxtacanalicular regions of the outflow tract.<sup>3,8</sup> Volume changes also can exert slower, more sustained effects on outflow resistance over hours through a cascade initiated by altering TM-cell release of adenosine triphosphate (ATP).<sup>9</sup> Swelling of TM cells

triggers release of ATP,<sup>9</sup> which in turn is converted to adenosine by ectoenzymes.<sup>10,11</sup> Adenosine then stimulates  $A_1$  adenosine receptors to secrete metalloproteinases MMP-2<sup>12</sup> and MMP-9.<sup>10</sup> These metalloproteinases reduce outflow resistance.<sup>13,14</sup> The mechanism appears likely to be a rearrangement of the funneling of fluid destined for outflow by rearranging the morphology of the juxtacanalicular tissue and inner endothelial wall.<sup>8</sup> To the extent that  $\text{Ca}^{2+}$ -activated  $\text{Cl}^-$  channels (CaCCs) regulate TM cell volume,<sup>15</sup> these channels would be highly relevant for addressing glaucoma.

Cell volume regulation strongly depends on the swelling- and stretch-activated  $\text{Cl}^-$  channel ( $I_{\text{Cl,Swell}}$ , also known as VRAC, VSOR, VSOAC) in most cells<sup>16</sup> and specifically in human TM cells.<sup>17</sup> Following anisomotic swelling, release of  $\text{Cl}^-$  through  $I_{\text{Cl,Swell}}$  and  $\text{K}^+$  through parallel  $\text{K}^+$  channels drives water release, as well, restoring cell volume to isosmotic levels (regulatory volume decrease [RVD]). Chloride ion release through swelling-activated channels also releases organic osmolytes, such as taurine.<sup>18</sup> Trabecular meshwork cells display an RVD, both as isolated cells<sup>17</sup> and in intact human outflow

TABLE. Custom-Made Anoctamin Primers for RT-PCR

Target	Forward Primer	Reverse Primer	Product, bp	Annealing Temp
<i>bAno1</i>	CCTCACGGGCTTTGAAGAG	CTCCAAGACTCTGGCTTCGT	75	55°C
<i>bAno2</i>	TGGATGTGCAACAATTGAAGA	GCATTCTGCTGGTCACACAT	59	55°C
<i>bAno3</i>	TCAGAGCAGAAGGCTTGATG	AAACATGATATCGGGGCTTG	61	54°C
<i>bAno4</i>	TGACTGGGATTTGATAGACTGG	GCTTCAAACCTGGGGTCGTAT	60	54°C
<i>bAno5</i>	TGGAAACATTAAAGAAGCCATTTA	GAGTTTGTCCGAGCTTTTTCG	72	54°C
<i>bAno6</i>	AGGAATGTTTTGCTACAAATGGA	GTCCAAGGTTTTCCAACACG	72	55°C
<i>bAno7S</i>	GGCTCTTACGGGAGCACAG	CAAACGAGGACGAAGTCGAT	106	55°C
<i>bAno7L</i>	GCTCTGTGGTGATCGTGGT	GGCACGGTACAGGATGATAGA	71	55°C
<i>bAno8</i>	GGAGGACCAGCCAATCATC	TGCTCGTGGACAGGGAAC	72	55°C
<i>bAno9</i>	CAAACCCAGCTGGAACCTC	GGATCCGGAGGCTCTCTT	60	54°C
<i>bAno10</i>	CAGGGTCTTCAAACGTCCAT	TCATCGTTTTCAAAGCCAACCT	73	55°C

tissue.<sup>19</sup> Studies using genome-wide RNAi screens have demonstrated that heteromers A, C, D, and E of the Leucine-Rich Repeat-Containing Protein 8 (LRRC8A,C,D,E) form an essential component of  $I_{Cl,Swell}$ .<sup>18,20</sup> Published evidence also suggests that a 10-member vertebrate family of calcium-activated anoctamins, Ano1-10 (*TMEM16* genes A-K) has an important role in cell volume regulation in other cells.<sup>15</sup> Agreement as to the role of anoctamins in cell volume regulation is incomplete, particularly since family members display several functions,<sup>21</sup> reportedly acting as CaCCs,<sup>22-32</sup> nonselective cation channels,<sup>33</sup> and scramblases or scramblase components, dissipating the phospholipid asymmetry across the plasma membrane.<sup>34,35</sup> Ano1<sup>22-24,36,37</sup> and Ano2<sup>24,36,37</sup> were the first and most clearly documented anoctamins to be CaCCs. More recently, Ano6 also has been demonstrated to function as an ion channel or channel component.<sup>28,29,33,38</sup> In contrast, Schreiber et al.<sup>38</sup> have reported that Ano9 and Ano10 expressed in Fisher Rat Thyroid (FRT) cells inhibit  $Ca^{2+}$ -activated  $Cl^-$  currents. However, the relative  $Na^+$  to  $Cl^-$  permeability ( $P_{Na}/P_{Cl}$ ) of Ano6 has been uncertain. In HEK293T cells overexpressing human Ano6, Shimizu et al.<sup>29</sup> found that Ano6 functioned exclusively as an anion channel, whereas Grubb et al.<sup>28</sup> reported that  $P_{Na}/P_{Cl} = 0.3$ . In contrast, Yang et al.<sup>33</sup> found that endogenous Ano6 in axolotl oocyte membranes and WT mouse megakaryocytes, as well as overexpressed mouse Ano6 in *Xenopus* oocyte membranes, acted as a nonselective cation channel ( $P_{Na}/P_{Cl} \sim 7$ ).

In part, conflicting reports likely reflect known interactions of anoctamins with other anoctamins and other channels (Discussion) which may modify anoctamin function differentially in other cells, tissues, and organs. In addition, much information concerning anoctamins derives from overexpression in cell lines or oocytes. Thus, it currently is impossible to predict from published studies of other cells the potential role of anoctamin channels in TM cells.

Given the strong link between TM-cell volume regulation and outflow resistance, the potential role of anoctamins in outflow regulation, and the conflicting results obtained with other cells, we have tested whether anoctamins modulate the  $Ca^{2+}$ -activated currents,  $I_{Cl,Swell}$ , and RVDs of human TM cells in primary culture and transformed cell lines of normal and glaucomatous origin. The results suggested that Ano6 modulates TM-cell volume regulation, an observation of potential relevance in targeting outflow resistance.

## MATERIALS AND METHODS

### Cellular Models

Transformed normal human TM cells (TM5) and glaucomatous TM cells (GTM3; both gracious gifts from Alcon Research, Inc.,

Fort Worth, TX, USA)<sup>39</sup> were maintained in Dulbecco's modified Eagle's medium (DMEM) high-glucose media supplemented with 10% fetal bovine serum, 2 mM L-glutamine, and 50  $\mu$ g/ml of gentamicin at 37°C in a humidified atmosphere of 5%  $CO_2$  and 95% air.<sup>11</sup> The glaucomatous GTM3 cells were studied in view of the relevance of CaCC cells to glaucoma (Introduction). Culture media were replaced every 3 days and cells subcultured 1:5 when reaching 90% confluence. Transformed normal human TM cells were studied in passages 20 to 38 and GTM3 cells in passages 23 to 102. Primary human TM cells (HTM)<sup>38</sup> were kept in DMEM low-glucose media with the same supplements; cells studied were from passages 4 to 7.<sup>40</sup> All reagents for cell culture were purchased from Gibco, Invitrogen (Carlsbad, CA, USA).

### Reverse Transcription-PCR (RT-PCR)

Total RNA was isolated from cells with the RNeasy Mini Kit (Qiagen, Valencia, CA, USA) and was treated with RNase-free DNase I to avoid possible contamination with genomic DNA. Reverse-transcription into cDNA then was performed with Taqman Reverse Transcription Reagents (Applied Biosystems [ABI], Foster City, CA, USA) following the manufacturer's instructions.<sup>9</sup> Polymerase chain reaction was performed with the AccuPrime Taq DNA polymerase High Fidelity Kit (Invitrogen) under the recommended conditions. Primers used for gene-specific amplification are shown in the Table. Polymerase chain reaction products were separated on 1% agarose gels containing 0.05% ethidium bromide. Bands were visualized under ultraviolet light, sized, and photographed by the Molecular Imager Gel Doc XR+ System (Bio-Rad, Hercules, CA, USA).

### Real-Time Quantitative PCR (qPCR)

Cell cDNA templates were obtained as noted in the previous paragraph. The TaqMan gene expression assay was conducted at least in triplicate for each cDNA sample. TaqMan qPCR assays were done in 96-well plates with TaqMan 2X PCR Master Mix (P05837; ABI) using 7300 Real-Time PCR System (ABI) and default thermocycler program. Inventoried FAM-labeled MGB TaqMan probes for Ano1, Ano2, and Ano6 used in the assays were Hs00216121\_m1, Hs00220570\_m1, and Hs03805835\_m1, respectively. The expression levels of indicated genes were calculated by the  $2^{-\Delta\Delta Ct}$  method, with human glyceraldehyde 3-phosphate dehydrogenase (GAPDH; Hs99999905\_m1, ABI) as the endogenous control.

### Transient siRNA Knockdown of Ano6

Trabecular meshwork cells (0.2 million) were plated in the growth media specified above with serum, but without

antibiotics, into 6-well tissue culture plates. After reaching 60% to 80% confluence, cells were transfected with siRNA directed against human Ano6 (20-60 pmol, sc-96071; Santa Cruz Biotechnology, Inc., Santa Cruz, CA, USA) using lipofectamine 2000 (Invitrogen). Control cells were transfected with scrambled RNA. Experimental and control cells were studied after reaching 90% confluence 48 hours later. Efficacy of transient knockdown was determined by qPCR.

### Western Immunoblotting

Cells were lysed with RIPA buffer (Pierce, Rockford, IL, USA) supplemented with protease inhibitor cocktail (Complete Mini Tablets; Roche Diagnostics, Indianapolis, IN, USA).<sup>11</sup> The samples were sonicated for 30 seconds with a 50% pulse and cleared by centrifugation (10,000g) at 4°-8°C for 30 minutes. Supernatant protein concentrations were measured with bicinchoninic acid (BCA) protein assay reagent (Pierce). Homogenate containing 20 µg protein/lane was separated by SDS-PAGE and transferred to polyvinylidene fluoride membranes (Millipore, Billerica, MA, USA). Nonspecific binding was blocked with Protein-Free Blocking Buffers (Pierce) for 1 hour. Blots then were incubated overnight at 4°-8°C with primary antibodies, followed by 1-hour incubations with secondary antibodies conjugated to horseradish peroxidase (HRP), and finally developed by chemiluminescence detection (Super-Signal WestPico Substrate; Pierce). The primary antibodies used were to: Ano1 (rabbit polyclonal antibody ab72984, 1/500; Abcam, Cambridge, MA, USA); Ano6 (rabbit polyclonal antibody SC-136930, 1/100; Santa Cruz Biotechnology, Inc.); and GAPDH (mouse monoclonal antibody ab8245, 1/10,000; Abcam). Secondary sheep anti-mouse and goat anti-rabbit IgG-HRP antibodies (1/8000) were purchased from Amersham (GE Healthcare LifeScience, Buckinghamshire, UK).

### Whole-Cell Patch Clamp

As previously described,<sup>41,42</sup> TM cells were trypsinized, resuspended, and allowed to settle on glass coverslips. Ruptured-patch, whole-cell currents in TM cells were measured with a MultiClamp 700B amplifier (Axon Instruments, Foster City, CA, USA) coupled to an external Bessel filter (model 900; Frequency Devices, Haverhill, MA, USA).

Micropipettes were prepared from Corning No. 7052 glass (World Precision Instruments [WPI], Sarasota, FL, USA) with a Flaming/Brown micropipette puller (P-97; Sutter Instruments Co., Novato, CA, USA), coated with Sylgard (WPI), and fire-polished with a microforge (MF-830; Narishige, Tokyo, Japan). Micropipette resistances were 2 to 4 MΩ, attaining several gigohms after seal formation. Potentials were measured in a perfusion chamber connected to a Ag/AgCl pellet in 3M KCl solution through a 3M KCl agar bridge. Step changes in potential from a holding potential (Vh) of 0 mV to values from +100 to -100 mV were applied in 20 mV decrements for 300 ms at 2-second intervals.

Data were recorded with a digital interface (Digidata 1322A; Molecular Devices, Union City, CA, USA) at 2 to 5 kHz and filtered at 500 Hz coupled with pClamp 9.2 software (Axon Instruments, Union City, CA, USA). Analysis was performed with the Clampfit 9.2 software (Axon Instruments). Unless otherwise stated, stimulations of current were measured at the maximum responses and inhibitions at the lowest values following drug application.

The micropipette filling solution contained (in mM): 24.2 NaCl, 110 aspartic acid, 120 N-methyl-D-glucamine base, 0.38 CaCl<sub>2</sub>, 0.8 NaHEPES, 11.2 HEPES, 1.0 EGTA, 1.0 MgATP, and 0.01 GTP (~280 mosmol/kg H<sub>2</sub>O, adjusted to pH 7.2). The isotonic bath contained (in mM): 110 NaCl, 6 HEPES, 6

NaHEPES, 1.8 CaCl<sub>2</sub>, 1.2 MgCl<sub>2</sub>, 5 glucose, and 67 mannitol (~310 mosmol/kg H<sub>2</sub>O, adjusted to pH 7.4). Swelling-activated Cl<sup>-</sup> currents (I<sub>Cl,swell</sub>) were generated by removing the mannitol from the bath solution, reducing the osmolality to approximately 240 mosmol/kg H<sub>2</sub>O at pH 7.4.

### Cell Volume by Electronic Cell Sizing

Cell volume was monitored by electronic cell sizing using a Coulter counter (ZBI-Channelyzer II; Beckman Coulter, Inc., Brea, CA, USA) with a 100 µm aperture.<sup>43</sup> Transformed normal human TM cells were trypsinized and resuspended in isotonic solutions with or without drugs for 1 hour. The isotonic bath comprised (in mM): 110 NaCl, 15 HEPES, 2.5 CaCl<sub>2</sub>, 1.2 MgCl<sub>2</sub>, 4.7 KCl, 1.2 KH<sub>2</sub>PO<sub>4</sub>, 30 NaHCO<sub>3</sub>, and 10 glucose (~300 mOsm/kg H<sub>2</sub>O, adjusted to pH 7.4). Thereafter, osmolality was reduced nearly 50% by lowering the NaCl concentration to 30.5 mM. The ensuing RVD was monitored by measuring cell volume at the time points indicated.

### Intracellular Ca<sup>2+</sup> Concentration by Fura-2

For measurements of free intracellular Ca<sup>2+</sup> activity, cells grown on coverslips for 1 day were loaded in the dark with 5 µM fura 2-AM and 0.01% Pluronic F-127 (Molecular Probes, Eugene, OR, USA) for 60 minutes at room temperature and perfused with fura-free solution for 30 minutes before data acquisition was begun.<sup>17</sup> Coverslips were mounted on a Nikon Diaphot microscope and visualized with a ×40 oil-immersion fluorescence objective. The emitted fluorescence (520 nm) from approximately 75 cells at approximately 90% confluence was sampled at 1 Hz with the photomultiplier following excitation at 340 and 380 nm, and the ratio was determined with a Delta-Ram system and Felix software (Photon Technology International, Edison, NJ, USA). The ratio (R) of light excited at 340 nm to that at 380 nm was taken to be a direct index of free intracellular Ca<sup>2+</sup> activity. That ratio was converted into free intracellular Ca<sup>2+</sup> concentration with the method of Grynkiewicz et al.<sup>44</sup> An in situ Kd value for fura 2 of 350 nM was used.<sup>45</sup> The minimal ratio value (R<sub>min</sub>) was obtained by bathing cells in a Ca<sup>2+</sup>-free isotonic solution of pH 8.0 containing 10 mM EGTA and 10 µM ionomycin. The maximal ratio value (R<sub>max</sub>) was obtained by bathing the cells in isotonic solution with 100 µM Ca<sup>2+</sup> and 10 µM ionomycin. Calibration was performed separately for each experiment. Baseline levels from TM cells in the absence of fura 2 were subtracted from control records to correct for autofluorescence.

### Statistics

Unless otherwise stated, Student's *t*-test was applied to compare two sets of data, and 1-way ANOVA was used for comparing three or more sets of data.<sup>11</sup> using the Holm-Sidak Multiple Comparison Procedure. Statistical analyses were conducted with SigmaStat (Aspire Software International, Ashburn, VA, USA). Results are presented as means ± SE, with *N* indicating the number of entries in the data set. A probability (*P*) less than 0.05 was considered statistically significant.

## RESULTS

### Anoctamin Expression

Of the three anoctamins (Ano1, Ano2, and Ano6) most convincingly associated with plasma membrane ion currents,<sup>24,46</sup> Ano6 was most strongly detected by RT-PCR of mRNA from human TM5 cells. In the representative RT-PCR

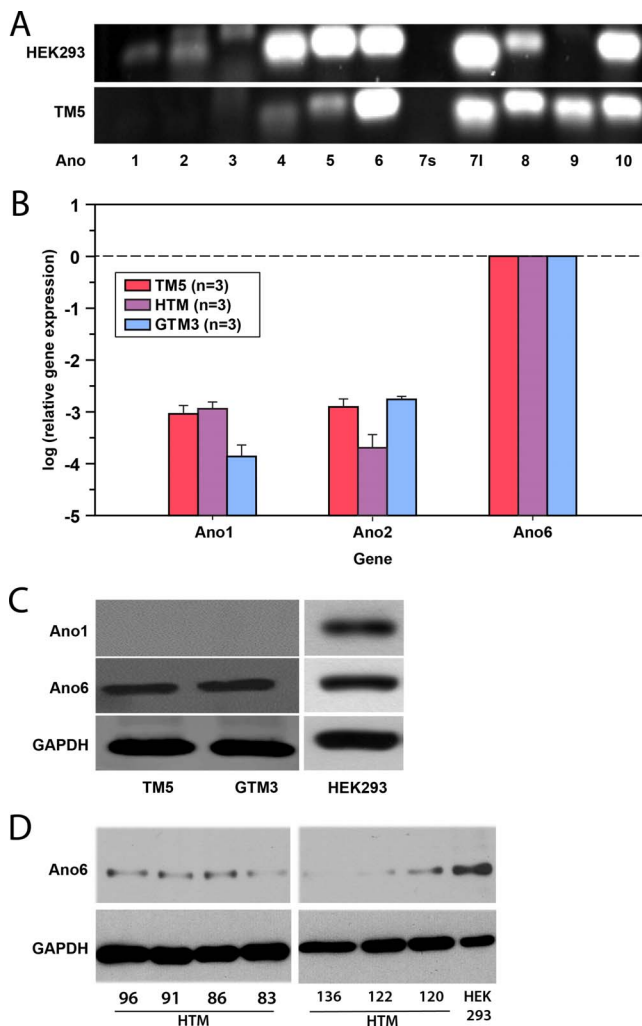


**FIGURE 1.** Expression of anoctamins in human TM cells at mRNA and protein levels. (A) Presents the gene expression of all human anoctamin isoforms An<sub>o</sub>1–An<sub>o</sub>10 (TMEM16A–K) from RT-PCR analyses ( $N = 3$ ) of TM5 and HEK293 cells. The expected product sizes are entered in the Table. An<sub>o</sub>7s is the short, and An<sub>o</sub>7l the long, splice variant of An<sub>o</sub>7 (TMEM16G). (B) Bar graphs display qPCR results indicating that TM5, HTM and GTM3 cells all express An<sub>o</sub>1 and An<sub>o</sub>2 three to four orders of magnitude lower than An<sub>o</sub>6. Protein expression of An<sub>o</sub>1 and An<sub>o</sub>6 isoforms in TM5, GTM3, and HEK293 cells were assayed by Western blots (C), while An<sub>o</sub> 6 protein expression in 7 different strains of human trabecular meshwork cells is shown in (D). An<sub>o</sub> 1 protein was not detected in these human TM cell strains (not shown). The sizes of An<sub>o</sub>1, An<sub>o</sub>6, and GAPDH were 114kDa, 106kDa, and 36kDa, respectively.

analysis of RNA from TM5 cells of Figure 1A ( $N = 3$ ), a strong band for An<sub>o</sub>6 was observed but An<sub>o</sub>1 and An<sub>o</sub>2 were not detected. Bands for all three genes, An<sub>o</sub>1, An<sub>o</sub>2, and An<sub>o</sub>6, were displayed for HEK293 cells, providing a positive control (Fig. 1A).

The relative gene expression of An<sub>o</sub>1, An<sub>o</sub>2, and An<sub>o</sub>6 in the TM cell lines and in primary cultures of HTM cells was quantitatively measured by qPCR. Each measurement was conducted in triplicate. The means  $\pm$  SE for three independent experiments are presented on the logarithmic ordinate scale of Figure 1B. The expression of An<sub>o</sub>6 was 3 to 4 orders of magnitude greater than that of either An<sub>o</sub>1 or An<sub>o</sub>2 in each of the three cell preparations. For example, the expressions of An<sub>o</sub>1 and An<sub>o</sub>2 relative to An<sub>o</sub>6 in HTM primary cultures were  $(1.2 \pm 0.4) \times 10^{-3}$  and  $(2 \pm 1) \times 10^{-4}$ , respectively. In the

absence of any dramatic difference in the relative expression of An<sub>o</sub>1 or An<sub>o</sub>2 to An<sub>o</sub>6 in GTM cells from a glaucomatous patient, we did not pursue further studies with GTM cells.

Western immunoblot (Fig. 1C) verified in two independent experiments that protein product of An<sub>o</sub>6, but not of An<sub>o</sub>1, was expressed by the TM5 and GTM3 cell lines, whereas both proteins were readily detectable with HEK293 positive controls. We next screened seven different primary HTM cell strains and observed An<sub>o</sub>6 protein expression in all studied (Fig. 1D).

### Anoctamins Regulate Ca<sup>2+</sup>-Triggered Plasma-Membrane Currents

In preliminary experiments ( $N = 4$ ), increasing the Ca<sup>2+</sup> concentration of the micropipette-filling solution to 15  $\mu$ M triggered currents, but only after a delay of approximately 10 minutes. In contrast, perfusion with 5  $\mu$ M ionomycin in the external bath raised intracellular Ca<sup>2+</sup> concentration to approximately 650 nM (Fig. 2A) and consistently elicited CaCC-like currents (Fig. 2B), usually within 20 seconds. Because of the consistency and rapidity of the response, ionomycin was thereafter applied to elicit Ca<sup>2+</sup>-activated currents. Ca<sup>2+</sup>-activated Cl<sup>-</sup> currents are characteristically outwardly-rectifying, displaying slow activation at highly positive intracellular potentials and deactivation at hyperpolarizing potentials.<sup>47</sup> Similar Ca<sup>2+</sup>-activated currents were observed in all TM cell preparations, comprising the TM5 and GTM3 cell lines and the HTM primary cultures.

The reversal potentials ( $E_{rev}$ ) of the currents activated in HTM and TM5 cells were positive. Measured 5 minutes after initiating ionomycin perfusion, the mean values of  $E_{rev} \pm$  SE (in mV) were  $12 \pm 1$  ( $N = 15$ ,  $P < 0.001$ ) and  $5 \pm 1$  ( $N = 8$ ,  $P = 0.002$ ) for HTM and TM5 cells, respectively. Reversal potentials were  $5 \pm 3$  ( $N = 7$ ) in GTM3 cells, not significantly different from zero ( $P = 0.141$ ). Probabilities were assessed by *t*-test after verifying normality by the Shapiro-Wilk test. The mean  $E_{rev}$  was significantly more positive for HTM cells than for TM5 ( $P = 0.015$ ) and GTM3 cells ( $P = 0.017$ ) by 1-way ANOVA, using the Holm-Sidak Multiple Comparison Procedure. Positive reversal potentials of ionomycin-activated currents are consistent with a dominant inflow of cations. For a positive control,  $E_{rev}$  of the swelling-activated Cl<sup>-</sup> currents ( $I_{Cl,swell}$ , Fig. 2C) at the same 5-minute endpoint was characteristically negative in TM cells, as previously reported.<sup>17</sup> In the present work, the  $E_{rev}$  values of  $I_{Cl,swell}$  were:  $-21 \pm 3$  ( $N = 13$ ,  $P < 0.001$ ),  $-14 \pm 4$  ( $N = 13$ ,  $P = 0.003$ ), and  $-19 \pm 3$  ( $N = 4$ ,  $P = 0.006$ ) for the HTM, TM5, and GTM3 cells, respectively. As for the ionomycin-activated currents,  $E_{rev}$  was measured approximately 5 minutes after hypotonic stimulation. The difference in  $E_{rev}$  between the ionomycin- and hypotonicity-stimulated currents was significant for each of the cell types, analyzed either by unpaired *t*-test when normality and equal variance were satisfied (GTM3 cells,  $P < 0.001$ ) or otherwise by the Mann-Whitney Rank Sum Test (HTM cells,  $P < 0.001$  and TM5 cells,  $P < 0.001$ ). Reversal potentials for  $I_{Cl,swell}$  were not significantly different from one cell type to another ( $P = 0.269$ , 1-way ANOVA).

The effects of two nonspecific CaCC inhibitors on the Ca<sup>2+</sup>-activated currents were measured after a baseline period of 5 minutes followed by ionomycin activation for 5 minutes before applying inhibitor. The percentage inhibitions after 5 minutes of exposure to inhibitor are presented in Figure 3A ( $N = 4$ –6). Both inhibitors reduced the Ca<sup>2+</sup>-activated currents, tannic acid > CaCC<sub>inh</sub>-A01<sup>48,49</sup> in TM5 and HTM cells. Tannic acid inhibits CaCC currents with an  $IC_{50}$  of 5.9  $\mu$ M in FRT-TMEM16A cells and 3.1  $\mu$ M in T84 cells (Fig. 3).<sup>49</sup> The CaCC<sub>inh</sub>-A01 inhibits CaCC currents with an  $IC_{50}$  of < 10  $\mu$ M in T84 cells (Fig. 7).<sup>48</sup> Tannic acid also inhibited the Ca<sup>2+</sup>-activated currents of GTM3

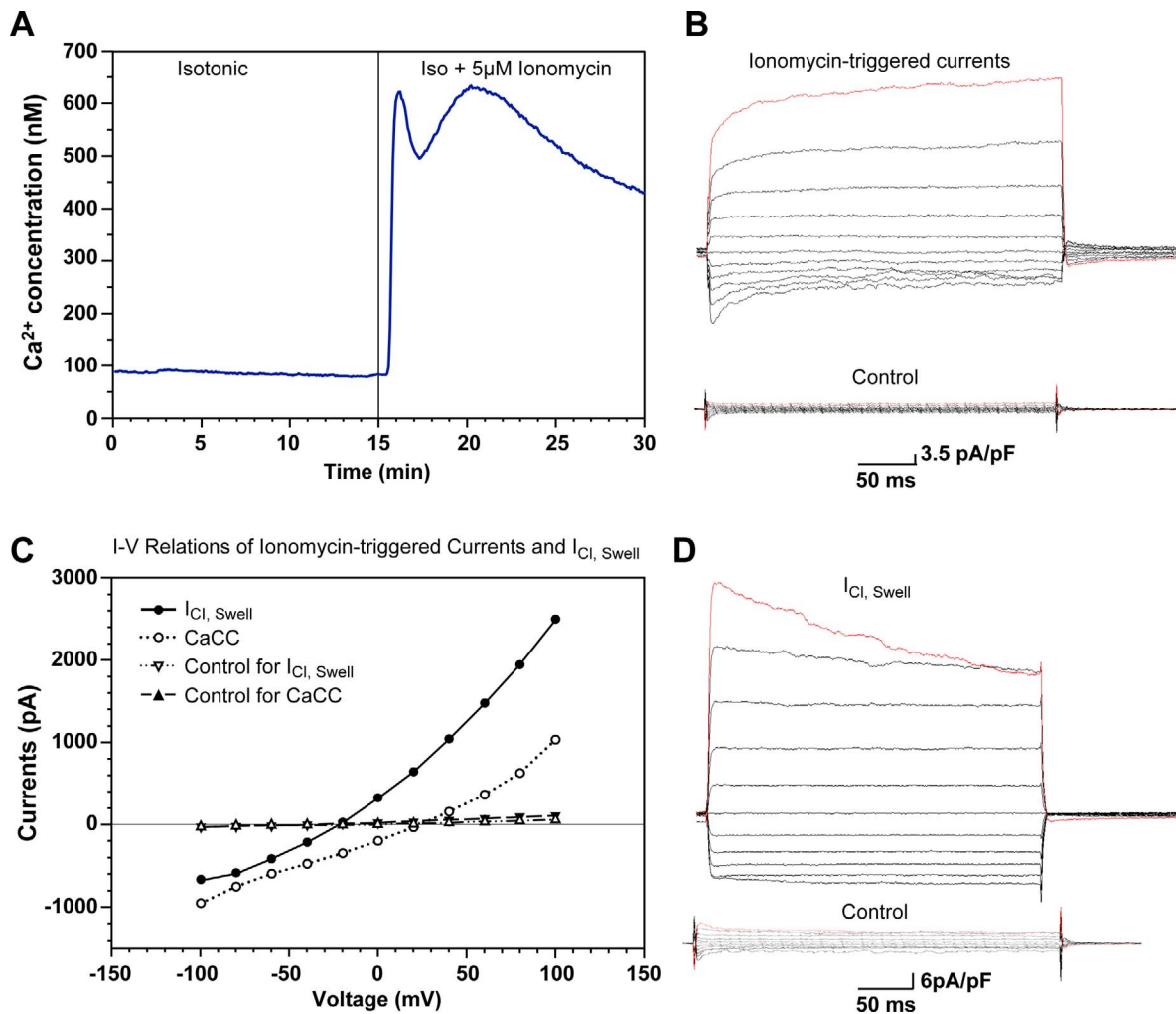


**FIGURE 2.** Effects of ionomycin and hypotonicity on TM-cell currents. **(A)** Displays the response of the free intracellular  $\text{Ca}^{2+}$  to perfusion with 5  $\mu\text{M}$  ionomycin. **(B)** Presents representative traces of baseline whole-cell perforated patch currents and currents measured 3 minutes after perfusing the TM5 cell with ionomycin. The currents are the responses to clamping the membrane potential at test pulses from +100 to -100 mV at decrements of 20 mV from a holding potential of 0 mV. The peak current reached 1647 pA at +100 mV, the nadir was -963 pA at -100 mV, and the membrane capacitance was 28 pF. The reversal potential was +25 mV, far from the  $\text{Cl}^-$  Nernst potential of -39 mV and consistent with activation of net cation inflow. **(D)** Illustrates representative baseline currents and swelling-activated ( $I_{\text{Cl,Swell}}$ ) currents 10 minutes after initiating hypotonic perfusion in another TM5 cell. The peak current reached 2491 pA at +100 mV, the nadir was -721 pA at -100 mV, and the membrane capacitance was 51 pF. The reversal potential was -21 mV, consonant with activation of net anion inflow. **(C)** Presents the current-voltage relationships for the experimental and baseline traces of **(B)** and **(D)**, measured 14 msec after the application of the test pulses.

cells (Fig. 3A;  $N = 5$ ). The effects of the CaCC inhibitors suggested that an anoctamin was subserving the  $\text{Ca}^{2+}$ -activated currents. The very high relative expression of Ano6 (Fig. 1B) pointed to that anoctamin as a likely conduit. This possibility was addressed by transient Ano6 knockdown (Fig. 3B). Knockdown efficiency was approximately  $69 \pm 15\%$  in this study. The knockdown reduced the  $\text{Ca}^{2+}$ -activated currents in TM5 ( $N = 8$ ,  $P = 0.002$ , unpaired  $t$ -test) and HTM cells ( $N = 4$ ,  $P = 0.02$ , unpaired  $t$ -test) by  $52 \pm 7\%$  and  $49 \pm 12\%$ , respectively, in comparison with the scrambled control cells.

### Role of Anoctamins in Regulating Plasma-Membrane Currents Triggered by Hypotonicity

In view of reports suggesting a role of anoctamins in cell volume regulation of other cells (Introduction), the CaCC inhibitors also were applied to hypotonically-activated TM cells. After a baseline period of 5 minutes followed by hypotonic activation for 10 minutes, inhibitions were assessed after exposure to: 100  $\mu\text{M}$  tannic acid for 2 minutes or 50  $\mu\text{M}$

CaCC<sub>inh</sub>-A01 for 10 minutes. The percentage inhibitions are presented in Figure 4A.

Reducing osmolality by approximately 23% triggered typical  $I_{\text{Cl,Swell}}$  currents<sup>16,17,50</sup> displaying modest outward rectification and time-dependent inactivation at highly depolarizing voltages (Figs. 2C, 2D). As in the case of the ionomycin-activated currents (Fig. 3A), tannic acid strongly reduced  $I_{\text{Cl,Swell}}$  in TM5, HTM, and GTM3 cells (Fig. 4A) in comparison with the scrambled controls. The nonselective inhibitor CaCC<sub>inh</sub>-A01 also reduced  $I_{\text{Cl,Swell}}$  in TM5 and HTM cells.

The effect of transient Ano6 knockdown on  $I_{\text{Cl,Swell}}$  also was examined in TM5 ( $N = 7$ ) and HTM ( $N = 5$ ) cells. As illustrated by Figure 4B, transient knockdown inhibited  $I_{\text{Cl,Swell}}$  of TM5 cells by  $73 \pm 11\%$  in comparison with the scrambled control cells ( $N = 5$ ,  $P = 0.028$ , unpaired  $t$ -test). Transient Ano6 knockdown of HTM cells also was associated with a trend to inhibition by  $54 \pm 19\%$  in comparison with scrambled controls ( $N = 4$ ). This trend did not reach significance ( $P = 0.054$ ). We have followed common convention in arbitrarily defining significance as a probability ( $P$ ) of the null hypothesis of

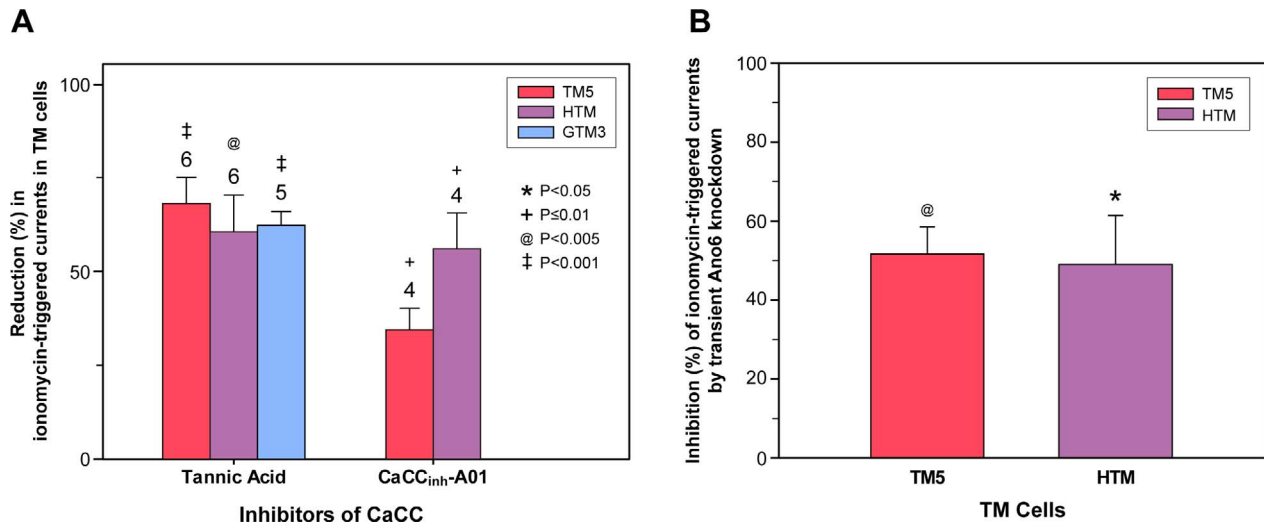


**FIGURE 3.** Effects of anoctamin inhibitors and transient Ano6 knockdown on ionomycin-triggered TM-cell currents. (A) Presents the percentage inhibition observed after 5 minutes of exposure of the ionomycin-activated TM cells to each inhibitor, 100  $\mu$ M tannic acid, or 50  $\mu$ M CaCC<sub>inh</sub>-A01, using each cell as its own series control. The numbers of cells studied are indicated over the corresponding bars. The data conformed to a normal distribution by the Shapiro-Wilk test. The probability of the null hypothesis was calculated by Student's *t*-test: \**P* < 0.05; †*P* < 0.01; @*P* < 0.005, and ‡*P* < 0.001. The symbols have the same significance in Figures 4 and 5, and are so defined in Figures 4A and 5A, as well. (B) Presents the percentage inhibition produced by transient Ano6 knockdown of three TM5 or three HTM cells in comparison with corresponding numbers of scrambled control cells. The probabilities of the null hypothesis were calculated from unpaired *t*-tests after verifying normality by the Shapiro-Wilk test and equal variance.

<0.05. However, this is arbitrary practice. Taken together with the effects of the CaCC inhibitors noted above in this section, the data suggested that Ano6 does enhance I<sub>Cl,Swell</sub> in TM cells.

**Anoctamins Modulate Regulatory Volume Decrease of TM Cells**

The foregoing results suggested that anoctamins regulate I<sub>Cl,Swell</sub> (Discussion). However, the primary issue of physiologic importance was whether anoctamins modulate cell volume regulation. This issue was addressed more directly by monitoring the regulatory volume response to anisotonic swelling.

As illustrated by the control trajectories displayed in all four panels of Figure 5, reducing the osmolality of the perfusion

solution by approximately 50% produced cell swelling, peaking 4 minutes later. Thereafter, progressive release of solute, and secondarily water, over the subsequent 26 minutes restored cell volume to within 1% to 6% of the initial isotonic volume. This RVD of TM cells primarily arises from K<sup>+</sup> and Cl<sup>-</sup> channels.<sup>17</sup>

Tannic acid, the more efficacious of the nonselective anoctamin blockers in inhibiting Ca<sup>2+</sup>-activated currents and I<sub>Cl,Swell</sub>, significantly slowed the RVD of the HTM and TM5 cells (Figs. 5A, 5B; *P* < 0.05, 1-way ANOVA at 30 minutes using the Holm-Sidak Multiple Comparison Procedure). The less efficacious nonselective anoctamin blocker CaCC<sub>inh</sub>-A01 displayed a trend to slow the RVD, which did not reach significance.

Transient Ano6 knockdown also slowed the RVD of TM5 and HTM cells. In comparison with the scrambled controls (*N*

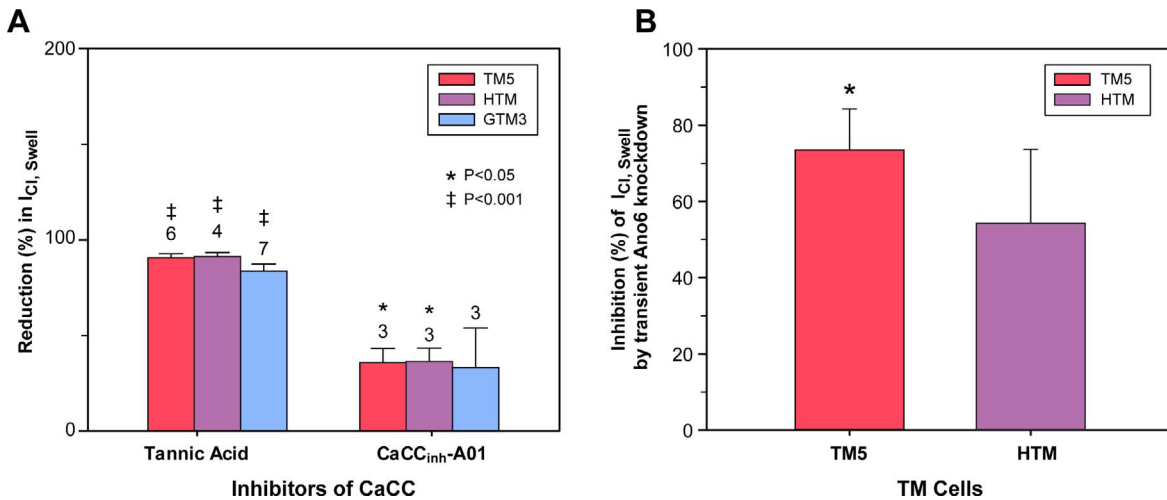


**FIGURE 4.** Effects of anoctamin inhibitors and transient Ano6 knockdown on hypotonicity-triggered TM-cell currents. After hypotonically triggering I<sub>Cl,Swell</sub>, perfusion with 100  $\mu$ M tannic acid or 50  $\mu$ M CaCC<sub>inh</sub>-A01 produced the inhibitions indicated by the bar graphs of (A). In general, the data were normally distributed by the Shapiro-Wilk test, permitting calculations of the probability of the null hypothesis with the *t*-test. These probabilities are indicated with the same symbols used in Figure 3. Transient Ano6 knockdown significantly inhibited I<sub>Cl,Swell</sub> of TM5 cells in comparison to the scrambled control cells (*N* = 5–7, *P* = 0.028) and displayed a trend to reduce those currents in HTM cells (*N* = 4–5, *P* = 0.054; [B]).

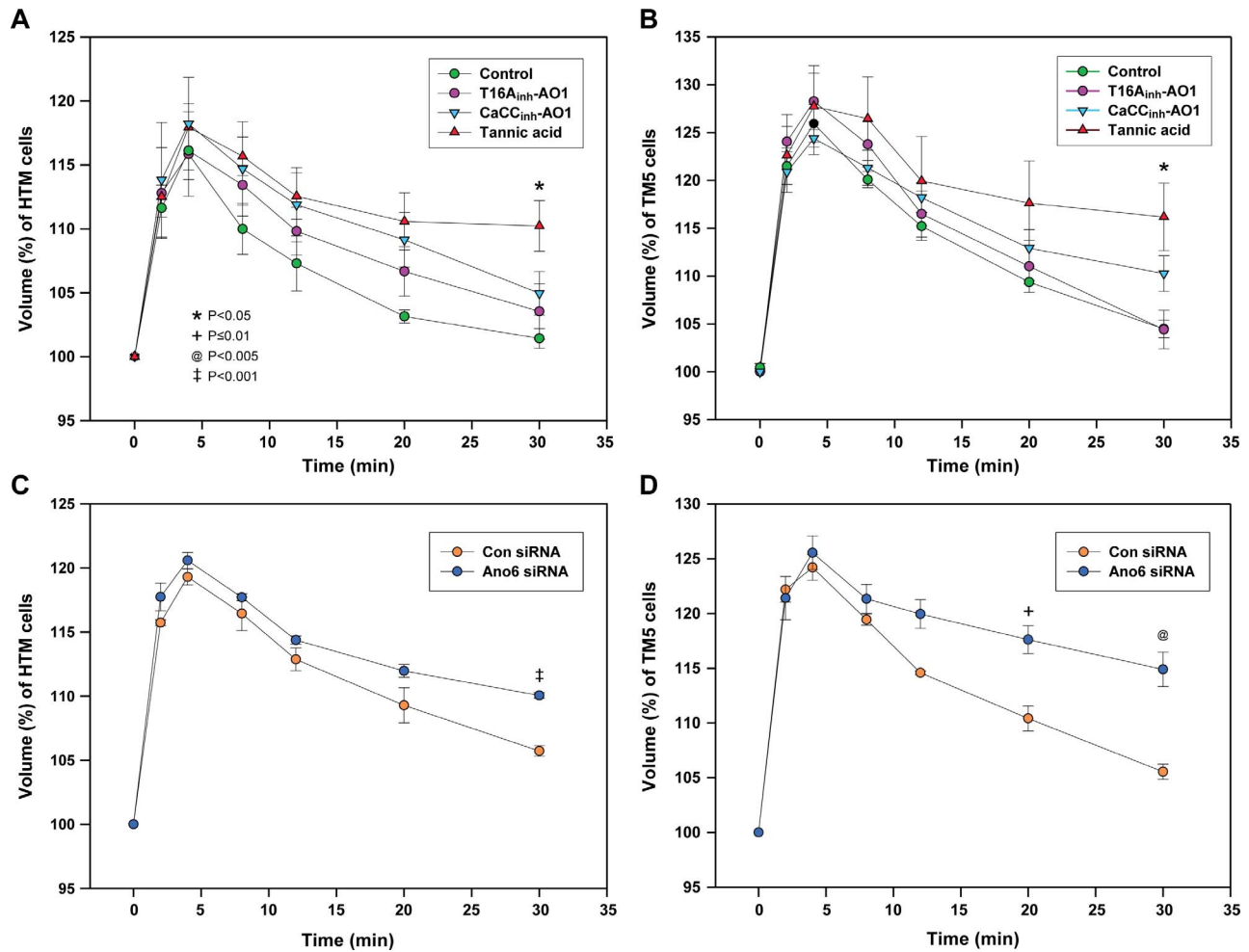


**FIGURE 5.** Effects of anoctamin inhibitors and transient Ano6 knockdown on RVD of TM cells. Halving the osmolality triggered swelling. Cell volume peaked 4 minutes later, followed by an RVD reflecting release of intracellular solute and water. Statistics were conducted either by 1-way ANOVA (A, B) or unpaired *t*-test (C, D) at each time point after first confirming that normality and equal variance were satisfied. The symbols indicate the same probabilities of the null hypothesis defined in Figure 3A, and are so defined in (A). Four experiments were averaged to generate the experimental trajectory of (D), and three experiments were averaged in generating the others. The nonselective CaCC inhibitor tannic acid slowed the control RVD of HTM cells (A) and TM5 cells (B). In both cases, TM cells remained significantly more swollen than the controls 30 minutes after applying hypotonicity. Similarly, transient Ano6 knockdown left the HTM cells (C) and TM5 cells (D) more swollen than the scrambled controls 30 minutes after establishing hypotonicity. The TM5 cells also remained more swollen at the 20-minute endpoint.

= 3), HTM cells with transient Ano6 knockdown ( $N = 3$ ) remained significantly larger 30 minutes after hypotonic exposure ( $P < 0.001$ , unpaired *t*-test, Fig. 5C). Following transient Ano6 knockdown, TM5 cells ( $N = 4$ ) remained larger than control cells ( $N = 3$ ) both 20 minutes ( $P = 0.010$ ) and 30 minutes ( $P < 0.001$ ) after applying hypotonicity (unpaired *t*-test, Fig. 5D).

The foregoing data obtained with CaCC inhibitors and transient Ano6 knockdown suggested that Ano6 enhances the RVD of human TM cells.

## DISCUSSION

### Relative Gene and Functional Expression of Ano1, Ano2, and Ano6

Of the 10-member vertebrate family of anoctamins, the three anoctamins clearly documented to subserve CaCCs in other cells are Ano1, Ano2, and Ano6 (Introduction). The current qPCR analyses indicated that gene expression of Ano6 in human TM cells is 3 to 4 orders of magnitude greater than

those of Ano1 and Ano2 (Fig. 1C). The RT-PCR analyses (Fig. 1A) and Western blots (Fig. 1B) are consistent with that observation. Nonselective inhibition of the anoctamins strongly inhibited all three functional assays. These observations suggested that an anoctamin, presumably Ano6, regulates TM-cell  $\text{Ca}^{2+}$ -activated currents,  $I_{\text{Cl,Swell}}$  and the RVD, an important physiologic regulator of TM cell volume and conventional outflow homeostasis.

### Ano6 Regulation of $\text{Ca}^{2+}$ -Activated Currents

In the presence of extracellular  $\text{Ca}^{2+}$ , the calcium ionophore ionomycin increased intracellular  $\text{Ca}^{2+}$  activity (Fig. 2A) and triggered membrane currents (Fig. 2B). The currents were modulated by Ano6, since they were reduced by nonselective CaCC inhibitors (Fig. 3A) and inhibited by partial transient Ano6 knockdown (Fig. 3B).

The macroscopic kinetics of the  $\text{Ca}^{2+}$ -activated currents were identical with those of  $\text{Ca}^{2+}$ -activated  $\text{Cl}^-$  currents.<sup>47</sup> However, the  $E_{\text{rev}}$  of the  $\text{Ca}^{2+}$ -activated currents ranged from +5 to +12 mV for the three TM cell types studied. In contrast,

$E_{rev}$  of the anion-selective channels  $I_{Cl,Swell}$  was clearly negative under the same experimental conditions, ranging from  $-14$  to  $-21$  mV for the same TM cell types. With the current solutions, the theoretical Nernst reversal potentials for  $Cl^-$  and  $Na^+$  were identical in magnitude but opposite in sign. Thus, the  $Ca^{2+}$ -activated currents of the TM cells reflect faster conduction of cation than anion, in contrast with human An6 currents homologously overexpressed in HEK293T cells<sup>29</sup> and mouse An6 heterologously overexpressed in HEK293 cells.<sup>28</sup> The current data suggested that  $P_{Na}/P_{Cl}$  was higher for  $Ca^{2+}$ -activated currents than  $I_{Cl,Swell}$  by 6.3-, 2.7-, and 3.8-fold for the HTM, TM5, and GTM3 cells, respectively. The present observations are most consonant with the endogenous An6 currents in axolotl oocyte membranes, reported to display a  $P_{Na}/P_{Cl}$  approximately 7 (Yang et al.<sup>39</sup>).

### Ano6 Regulation of Swelling-Activated $Cl^-$ Currents ( $I_{Cl,Swell}$ )

As widely observed with other cells, hypotonic swelling triggers  $I_{Cl,Swell}$  in TM cells (Fig. 2C) associated with the negative  $E_{rev}$  noted above (Section 4.2). Nonselective CaCC inhibitors inhibited  $I_{Cl,Swell}$  in these cells (Fig. 4A) and transient Ano6 knockdown also strongly inhibited  $I_{Cl,Swell}$  in TM5 TM cells (Fig. 4B). The RVD, which depends upon  $I_{Cl,Swell}$ , also was inhibited by the nonselective CaCC inhibitor tannic acid and by transient Ano6 knockdown in TM5 and HTM cells (Fig. 5).

Almaça et al.<sup>7</sup> first reported that selective transient knockdown of anoctamins 1, 6, 8, and 9 nonadditively reduced the whole-cell conductance of hypotonically-activated HEK293 cells. In contrast, Shimizu et al.<sup>29</sup> found that selective transient knockdown of either Ano6 or Ano10 had no effect on the current-voltage relationship of  $I_{Cl,Swell}$  in HEK293T and HeLa cells. Juul et al.<sup>46</sup> have emphasized that the effects displayed by manipulating Ano6 strongly depend on the presence of extracellular  $Ca^{2+}$ . The latter investigators found that the RVD of Ehrlich ascites tumor cells was unaffected by stable Ano6 knockdown in the total absence of external  $Ca^{2+}$ , but was strongly inhibited in the presence of 0.5 mM  $Ca^{2+}$ . However, differences in bath  $Ca^{2+}$  are unlikely to account for the divergent results reported by Shimizu et al.<sup>29</sup> External  $Ca^{2+}$  was present in the solutions of Almaça et al.<sup>7</sup> (1.3 mM calcium gluconate) and Shimizu et al.<sup>29</sup> (2 mM  $CaSO_4$  in baseline solutions). In the present work, 1.8 mM  $CaCl_2$  was included in the external bath.

The mechanism by which Ano6 modulates  $I_{Cl,Swell}$  cannot be identified from our data. The pore of  $I_{Cl,Swell}$  is formed by LRRC8 heteromers.<sup>51</sup> Isomers A, C, D, and E of the LRRC8 family are incorporated in the channel.<sup>16,17</sup> The specific isomeric configuration determines  $I_{Cl,Swell}$  inactivation kinetics,<sup>16</sup> and the isomeric combination varies with cell type.<sup>16</sup> Whether or not Ano6 interacts directly with LRRC8A,C,D,E in other cells is unknown. However, anoctamins do interact with other anoctamins as hetero-oligomers<sup>27,38,52</sup> and with other channels, such as CFTR,<sup>26</sup> TRPC2,<sup>53</sup> and TRPV4,<sup>54</sup> which may modulate anoctamin function variably in different cells and tissues.

### Future Implications

The current results may well have clinical implications. The autocrine release of ATP that initiates purinergic regulation of outflow can be triggered equally well by hyposmotic swelling or cell stretch.<sup>10</sup> The duration of the stimulus determines the amount of ATP released, and, thus, the amount of MMP-2 and MMP-9 released downstream. The physiologic event that terminates ATP release is the RVD, which permits the TM cells to restore their baseline volumes, thereby removing the

signal for ATP release. Early restoration of osmolality by adding mannitol terminates the period of ATP release. Pretreatment with dexamethasone also accelerates the RVD, reducing the period of ATP and MMP release.<sup>10</sup> In contrast, slowing the RVD with cytochalasin prolongs the period of cell stress and thereby increases ATP and downstream MMP secretion.<sup>10</sup> Our data indicated that Ano6 accelerates the RVD, reducing the period for ATP and MMP release. These results raise the possibility of pharmacologically targeting Ano6 or its link to LRRC8, the critical component of  $I_{Cl,Swell}$ . Inhibiting the action of Ano6 is expected to maintain the TM cell volume high, thereby enhancing the rate of ATP release and further reducing outflow resistance. It should be noted that a larger percentage inhibition of ionomycin-triggered currents and  $I_{Cl,Swell}$  was noted with nonspecific inhibitors than by Ano6 siRNA knockdown. This suggests that anoctamins in addition to Ano6 may have a role in TM cell volume regulation. The possibility of targeting Ano6 to modify TM cell volume, suggested by our studies of cultured cells, is supported by recent exon-level expression profiling of Ano6 in 10 ocular tissues.<sup>55</sup> The data can be accessed at <https://genome.uiowa.edu/otdb/search?type=symbol&term=ANO6&set=extended>, in the public domain. Not only is Ano6 expressed far more than any other trabecular meshwork anoctamin, but Ano6 is more highly expressed in trabecular meshwork than in the other 9 ocular tissues tested. Development of this novel approach for lowering IOP will require future identification of the LRRC8 isomers expressed by normal and glaucomatous TM cells, and the mechanism(s) of interaction between LRRC8 and Ano6 in human TM cells.

### Acknowledgments

The authors thank Gui-shuang Ying (Biostatistics Module, Penn Vision Research Center, University of Pennsylvania, Philadelphia, PA, USA), Terry Braun (Coordinated Laboratory for Computational Genomics, Biomedical Engineering, University of Iowa, Iowa City, IA, USA), and Abbot F. Clark (North Texas Eye Research Institute, University of North Texas Health Science Center, Ft. Worth, TX, USA) for helpful discussions; and Kristin PerkuJunimas (Department of Ophthalmology, Duke University, Durham, NC, USA) for help with immunoblotting.

Supported by National Institutes of Health (NIH; Bethesda, MD, USA) Research Grant EY13624 and Core Grant EY01583 (M.M.C.).

Disclosure: **J. Banerjee**, None; **C.-T. Leung**, None; **A. Li**, None; **K. Peterson-Yantorno**, None; **H. Ouyang**, None; **W.D. Stamer**, None; **M.M. Civan**, None

### References

- Grant WM. Clinical measurements of aqueous outflow. *Arch Ophthalmol*. 1951;46:113-131.
- Brubaker RF. Clinical measurements of aqueous dynamics: implications for addressing glaucoma. In: Civan MM, ed. *Eye's Aqueous Humor: From Secretion to Glaucoma. Current Topics in Membranes*. San Diego: Academic Press; 1998:45:1-24.
- Stamer WD. The cell and molecular biology of glaucoma: mechanisms in the conventional outflow pathway. *Invest Ophthalmol Vis Sci*. 2012;53:2470-2472.
- Clark AF. The cell and molecular biology of glaucoma: biochemical factors in glaucoma. *Invest Ophthalmol Vis Sci*. 2012;53:2473-2475.
- Rohen JW. Experimental studies on the trabecular meshwork in primates. *Arch Ophthalmol*. 1963;69:335-349.
- Gual A, Llobet A, Gilabert R, et al. Effects of time of storage, albumin, and osmolality changes on outflow facility (C) of



- bovine anterior segment in vitro. *Invest Ophthalmol Vis Sci.* 1993;38:2165-2171.
7. Al-Aswad LA, Gong H, Lee D, et al. Effects of Na-K-2Cl cotransport regulators on outflow facility in calf and human eyes in vitro. *Invest Ophthalmol Vis Sci.* 1999;40:1695-1701.
  8. Overby DR, Stamer WD, Johnson M. The changing paradigm of outflow resistance generation: towards synergistic models of the JCT and inner wall endothelium. *Exp Eye Res.* 2009;88:656-670.
  9. Li A, Leung CT, Peterson-Yantorno K, et al. Mechanisms of ATP release by human trabecular meshwork cells, the enabling step in purinergic regulation of aqueous humor outflow. *J Cell Physiol.* 2012;227:172-182.
  10. Li A, Leung CT, Peterson-Yantorno K, et al. Cytoskeletal dependence of adenosine triphosphate release by human trabecular meshwork cells. *Invest Ophthalmol Vis Sci.* 2011;52:7996-8005.
  11. Li A, Banerjee J, Peterson-Yantorno K, et al. Effects of cardiostimulatory steroids on trabecular meshwork cells: search for mediator of ouabain-enhanced outflow facility. *Exp Eye Res.* 2012;96:4-12.
  12. Shearer TW, Crosson CE. Adenosine A1 receptor modulation of MMP-2 secretion by trabecular meshwork cells. *Invest Ophthalmol Vis Sci.* 2002;43:3016-3020.
  13. Bradley JM, Vranka J, Colvis CM, et al. Effect of matrix metalloproteinases activity on outflow in perfused human organ culture. *Invest Ophthalmol Vis Sci.* 1998;39:2649-2658.
  14. Crosson CE, Sloan CF, Yates PW. Modulation of conventional outflow facility by the adenosine A1 agonist N6-cyclohexyladenosine. *Invest Ophthalmol Vis Sci.* 2005;46:3795-3799.
  15. Almaça J, Tian Y, Aldehni F, et al. TMEM16 proteins produce volume-regulated chloride currents that are reduced in mice lacking TMEM16A. *J Biol Chem.* 2009;284:28571-28578.
  16. Hoffmann EK, Lambert IH, Pedersen SF. Physiology of cell volume regulation in vertebrates. *Physiol Rev.* 2009;89:193-277.
  17. Mitchell CH, Fleischhauer JC, Stamer WD, et al. Human trabecular meshwork cell volume regulation. *Am J Physiol Cell Physiol.* 2002;283:C315-C326.
  18. Voss FK, Ullrich F, Münch J, et al. Identification of LRRC8 heteromers as an essential component of the volume-regulated anion channel VRAC. *Science.* 2014;344:634-638.
  19. McLaughlin CW, Karl MO, Zellhuber-McMillan S, et al. Electron probe X-ray microanalysis of intact pathway for human aqueous humor outflow. *Am J Physiol Cell Physiol.* 2008;295:C1083-C1091.
  20. Qiu Z, Dubin AE, Mathur J, et al. SWELL1, a plasma membrane protein, is an essential component of volume-regulated anion channel. *Cell.* 2014;157:447-458.
  21. Kunzelmann K, Nilius B, Owsianik G, et al. Molecular functions of anoctamin 6 (TMEM16F): a chloride channel, cation channel, or phospholipid scramblase? *Pflugers Arch.* 2014;466:407-414.
  22. Yang YD, Cho H, Koo JY, et al. TMEM16A confers receptor-activated calcium-dependent chloride conductance. *Nature.* 2008;455:1210-1215.
  23. Caputo A, Caci E, Ferrera L, et al. TMEM16A, a membrane protein associated with calcium-dependent chloride channel activity. *Science.* 2008;322:590-594.
  24. Schroeder BC1, Cheng T, Jan YN, et al. Expression cloning of TMEM16A as a calcium-activated chloride channel subunit. *Cell.* 2008;134:1019-1029.
  25. Stephan AB, Shum EY, Hirsh S, et al. ANO2 is the ciliary calcium-activated chloride channel that may mediate olfactory amplification. *Proc Natl Acad Sci U S A.* 2009;106:11776-11781.
  26. Martins JR, Faria D, Kongsuphol P, Reisch B, Schreiber R, Kunzelmann K. Anoctamin 6 is an essential component of the outwardly rectifying chloride channel. *Proc Natl Acad Sci U S A.* 2011;108:18168-18172.
  27. Tian Y, Schreiber R, Kunzelmann K. Anoctamins are a family of Ca<sup>2+</sup>-activated Cl<sup>-</sup> channels. *J Cell Sci.* 2012;125:4991-4998.
  28. Grubb S, Poulsen KA, Juul CA, et al. TMEM16F (Anoctamin 6), an anion channel of delayed Ca(2+) activation. *J Gen Physiol.* 2013;141:585-600.
  29. Shimizu T, Ichihara T, Sato K, et al. TMEM16F is a component of a Ca<sup>2+</sup>-activated Cl<sup>-</sup> channel but not a volume-sensitive outwardly rectifying Cl<sup>-</sup> channel. *Am J Physiol Cell Physiol.* 2013;304:C748-C759.
  30. Ousingsawat J, Wanitchakool P, Kmit A, et al. Anoctamin 6 mediates effects essential for innate immunity downstream of P2X7 receptors in macrophages. *Nat Commun.* 2015a;6:6245.
  31. Ousingsawat J, Wanitchakool P, Schreiber R, Wuelling M, Vortkamp A, Kunzelmann K. Anoctamin-6 controls bone mineralization by activating the calcium transporter NCX1. *J Biol Chem.* 2015b;290:6270-6280.
  32. Kim HJ, Jun I, Yoon JS, et al. Selective serotonin reuptake inhibitors facilitate ANO6 (TMEM16F) current activation and phosphatidylserine exposure. *Pflugers Arch.* 2015;467:2243-2256.
  33. Yang H, Kim A, David T, et al. TMEM16F forms a Ca<sup>2+</sup>-activated cation channel required for lipid scrambling in platelets during blood coagulation. *Cell.* 2012;151:111-122.
  34. Suzuki J, Fujii T, Imao T, et al. Calcium-dependent Phospholipid scrambling activity of TMEM16 family members. *J Biol Chem.* 2013;288:13305-13316.
  35. Suzuki J, Umeda M, Sims PJ, et al. Epub 2011 Nov 14. Calcium-dependent phospholipid scrambling by TMEM16F. *Nature.* 2010;468:834-838.
  36. Stöhr H, Heisig JB, Benz PM, et al. TMEM16B, a novel protein with calcium-dependent chloride channel activity, associates with a presynaptic protein complex in photoreceptor terminals. *J Neurosci.* 2009;29:6809-6818.
  37. Pifferi S, Dibattista M, Menini A. TMEM16B induces chloride currents activated by calcium in mammalian cells. *Pflugers Arch.* 2009;458:1023-1038.
  38. Schreiber R, Uliyakina I, Kongsuphol P, et al. Expression and function of epithelial anoctamins. *J Biol Chem.* 2010;285:7838-7845.
  39. Pang IH, Shade DL, Clark AF, et al. Preliminary characterization of a transformed cell strain derived from human trabecular meshwork. *Curr Eye Res.* 1994;13:51-63.
  40. Stamer WD, Sefror RE, Williams SK, et al. 1995. Isolation and culture of human trabecular meshwork cells by extracellular matrix digestion. *Curr Eye Res.* 1995;14:611-617.
  41. Karl MO, Fleischhauer JC, Stamer WD, et al. Differential P1-purinergic modulation of human Schlemm's canal inner-wall cells. *Am J Physiol Cell Physiol.* 2005;288:C784-C794.
  42. Karl MO, Peterson-Yantorno K, Civan MM. Cell-specific differential modulation of human trabecular meshwork cells by selective adenosine receptor agonists. *Exp Eye Res.* 2007;84:126-134.
  43. Yantorno RE, Coca-Prados M, Krupin T, et al. Volume regulation of cultured, transformed, non-pigmented epithelial cells from human ciliary body. *Exp Eye Res.* 1989;49:423-437.
  44. Gryniewicz G, Poenie M, Tsien RY. A new generation of Ca<sup>2+</sup> indicators with greatly improved fluorescence properties. *J Biol Chem.* 1985;260:3440-3450.
  45. Negulescu PA, Machen TE. Intracellular ion activities and membrane transport in parietal cells measured with fluorescent dyes. *Methods Enzymol.* 1990;192:38-81.

46. Juul CA, Grubb S, Poulsen KA, et al. Anoctamin 6 differs from VRAC and VSOAC but is involved in apoptosis and supports volume regulation in the presence of  $\text{Ca}^{2+}$ . *Pflugers Arch*. 2014;466:1899-1910.
47. Hartzell HC, Yu K, Xiao Q, et al. Anoctamin/TMEM16 family members are  $\text{Ca}^{2+}$ -activated  $\text{Cl}^-$  channels. *J Physiol*. 2009; 587:2127-2139.
48. De La Fuente R, Namkung W, Mills A, et al. Small-molecule screen identifies inhibitors of a human intestinal calcium-activated chloride channel. *Mol Pharmacol*. 2008;73:758-768.
49. Namkung W, Phuan PW, Verkman AS. TMEM16A inhibitors reveal TMEM16A as a minor component of calcium-activated chloride channel conductance in airway and intestinal epithelial cells. *J Biol Chem*. 2011;286:2365-2374.
50. Okada Y. Volume expansion-sensing outward-rectifier  $\text{Cl}^-$  channel: fresh start to the molecular identity and volume sensor. *Am J Physiol*. 1997;273:C755-C789.
51. Syeda R, Qiu Z, Dubin AE, et al. LRRC8 proteins form volume-regulated anion channels that sense ionic strength. *Cell*. 2016; 164:499-511.
52. Tien J, Lee HY, Minor DL Jr, et al. Identification of a dimerization domain in the TMEM16A calcium-activated chloride channel (CaCC). *Proc Natl Acad Sci U S A*. 2013; 110:6352-6357.
53. Viitanen TM, Sukumaran P, Löf C, et al. Functional coupling of TRPC2 cation channels and the calcium-activated anion channels in rat thyroid cells: implications for iodide homeostasis. *J Cell Physiol*. 2013;228:814-823.
54. Takayama Y, Shibasaki K, Suzuki Y, et al. Modulation of water efflux through functional interaction between TRPV4 and TMEM16A/noctamin 1. *FASEB J*. 2014;28:2238-48.
55. Wagner AH, Anand VN, Wang WH, et al. Exon-level expression profiling of ocular tissues. *Exp Eye Res*. 2013; 111:105-111.